Silikáty 32, s. 109—123 (1988)

THE EFFECT OF FIRING TEMPERATURE ON THE PROPERTIES OF MODEL THICK-FILM RESISTORS

I. Morphology and Microstructure of the Films

ALOIS KUBOVÝ, IVO HAVLAS

Research Institute of Electrotechnical Ceramics, Pospíšilova 281, 500 64 Hradec Králové

Received 18. 8. 1987

On the basis of microscopical examinations and resistivity and Seebeck's coefficient measurements, a model of the development of structure (morphology) of thick-film resistors (TFR) during their firing has been suggested. The model differs from those published so far particularly in that formation of a narrow band of localised impurity states, resulting from diffusion of Ru from the conductive grains, is considered instead of sintering of conductive grains in the last stage of structural development.

INTRODUCTION

Perfect knowledge of the effect of technological conditions on the properties of fired films is one of the prerequisites for continuing application of thick-film resistors (TFR) in hybrid integrated circuits (HIC) in view of the increasing demands on their parameters. The firing of the films is one of the decisive technological operations. The present study is the first of a series of several papers in which the authors strive to formulate a complex conception of the effect of firing parameters, particularly its peak temperature, on the properties of thick-film resistors. The additional papers will deal with the effect of firing temperature on the critical coefficients of the percolation theory, the effect of repeated firing on the properties of model resistor films and finaly with the relationships between the parameters of the glass frit employed and the behaviour of films in the course of firing.

Similarly to other types of thick layers, thick-film resistors are created by screen printing on insulating, particularly alumina substrates and subsequent firing in a tunnel kiln. After firing, the TFR represents an inequilibrial heterogeneous system based on two essential inorganic components, namely the conductive pigment and the glass. The initial pastes for screen printing also contain an organic vehicle. The conductive component mostly consists of oxidic compounds of ruthenium, namely RuO_2, or oxide compounds with cubic pyrochlor structure, particularly $Bi_2Ru_2O_7$ or $Pb_2Ru_2O_6$. The glass introduced into the paste in the form of a finely ground frit belongs typically to the system of high-lead silicate or borosilicate glasses. The inorganic component of commercial pastes used in the manufacture of HIC or potentiometers further contains modifiers, i.e. oxides of metals which adjust the course of the temperature dependence of sheet resistivity, or improve its long-term stability.

The sheet resistivity of typical TFR depends on volume concentration of the conductive component and varies over the range of 10 to 10^7 Ohm $\square^{-1}$, which at a film thickness of 15 μm corresponds to resistivities over the interval of 1.5×10^{-4} to 1.5×10^2 Ohm . m.

The properties of TFR are closely associated with their structure (morphology), i.e. with the arrangement of conductive and insulating (glass) grains in the film, or conductive grains in the continuous glassy matrix. The literature describes essentially two different types of TFR morphology. The first type described in [1, 2] was found in films based on RuO_2 and is characteristic of segregation of conductive pigment particles at the grain boundaries of the substantially larger sintered glass particles. This type of arrangement of conductive particles is called segregated structure. Approximately homogeneous distribution of conductive particles in the glass matrix was observed in [3] with TFR based on ruthenates with a pyrochlor structure. This type of arrangement is called quasihomogeneous structure. In this type of morphology, the distribution of conductive particles throughout the glassy matrix is often approximated by *sc* lattice arrangement with the latice parameter according to the equation [4]:

$$s = \left(\frac{\pi}{6v}\right)^{1/3} . d, \tag{1}$$

where v is the concentration of the conductive component by volume and d is the mean diameter of its grain. In addition to this, the two basic types of TFR structure can be combined with another type of segregation resulting from sedimentation of conductive grains towards the substrate [5]. The chemical reactions between the conductive component and glass, taking place during the firing, are discussed in [6]. According to this study, with the use of high-lead glasses and the $Bi_2Ru_2O_7$ conductive pigment, the firing reaction produces the mixed ruthenate $Bi_{2-x}Pb_xRu_2O_{7-x/2}$, and decomposition of $Bi_2Ru_2O_7$ yields RuO_2, while the bismuth oxide enters the glass. In the case of systems based on RuO_2 it is assumed that firing brings about formation of $Pb_2Ru_2O_6$ particularly at the surface of conductive grains.

The development of structure during firing and the mechanisms involved are described in [7—9, 15]. The structure is assumed to develop in the following stages [9]:

1. Sintering of glass and wetting of conductive particles.
2. Rearrangement of conductive particles and formation of the conductive lattice.
3. Sintering of conductive particles in the presence of glass.
4. Growth of the larger conductive particles at the expense of the smaller ones (Ostwald ripening).

However, the sintering of conductive particles was not proved directly [7—9], being only indicated by the growth of conductive grains observed at high temperatures and after relatively long periods of time. The effect of the firing process on the properties of TFR was the subject of several additional studies [10—12]; however, a complex conception of the structure of TFR and their properties has still been lacking. Moreover, some conceptions of the structural development, e.g. those suggested in [7—9], and in particular the process of sintering of conductive grains, are in disagreement with the results of other measurements [13]. A new conception of the development of structure in the course of firing will therefore be suggested in the present and subsequent articles.

MATERIALS

To simplify the subject matter, use was made of specimens prepared from model resistor pastes containing only the glass frit and the conductive pigment in its inorganic component. The model films containing either $Bi_2Ru_2O_7$ with a surface

area (measured by the Brunauer—Emmet—Teller method, BET) of 5 $m^2 g^{-1}$, or RuO_2 with a BET surface area of 8.9 $m^2 g^{-1}$, were studied. Similarly, only one of the two glasses (*A*, *B*), whose composition and surface area are listed in Table I,

Table I

Chemical composition and BET specific area of the powdered glasses

Glass designation	Composition (wt. %)				Specific area (m^2/g)
	PbO	SiO_2	B_2O_3	Al_2O_3	
A	66	32.5	—	1.5	1.05
B	69	22	7.5	1.5	2.10

were used in the experimental films. After grinding, a part of glass A was air classified in the Multiplex-Zickzacksichter 100 MR instrument made by Alpine Ausberg Co. The particle sizes of 3,5 and 10 μm were chosen as sorting limits. The classification produced 4 grain size fractions with BET surface areas of 2.24, 1.17, 0.78 and 0.51 $m^2 g^{-1}$ respectively. The value of specific area in brackets is given behind the letter *A* in the designation of the respective classified frit. The lacquer vehicle employed was based on ethylcellulose and terpineol. The type SA 305 08 substrates from TESLA Hradec Králové Concern Corporation contained 96 % Al_2O_3. The specimens of films for resistivity and Seebeck's coefficient measurements were of rectangular shape 12 × 2 mm^2 in size and 15 to 30 μm in thickness according to the maximum temperature of the firing cycle. The firing of the films was carried out in a tunnel kiln with a soaking time of 9 minutes at the maximum temperature. The maximum firing temperatures were chosen from the range of 450 to 900 °C.

EXPERIMENTAL METHODS

The structure (morphology) of the films was studied by optical microscopy in reflected light and by scanning electron microscopy (SEM). Polished surfaces of the films were examined, in the case of SEM, after selective etching according to [16] to achieve suitable contrast between the conductive component and the glassy matrix. The dependence of porosity on firing temperature was evaluated quantitatively by the automatic image analyzer IBAS-SEM-IPS made by Opton Corporation, in combination with an optical microscope.

The DC resistivity was measured with the Metra M1T 291 multimeter at room temperature. The thermoelectric voltage as well as the voltage of Pt—PtRh10 thermocouples for the determination of the temperature difference were measured with the same multimeter with an accuracy better than 1 μV. A correction for thermoelectric voltage of the Pt leads was carried out in the calculation of Seebeck's coefficient α_{abs}.

EXPERIMENTAL RESULTS

In the present part, the results will be given of studying the morphology by optical and scanning electron microscopy, examination of the microstructure of crystalline components by X-ray diffraction and by area resistivity measurements at room temperature on specimens fired at various peak temperatures t_v from the interval of 450 to 900 °C.

Morphology of the films

The development of the morphology of films in the course of firing can be seen in Figs. 1 and 2 which are optical micrographs (magn. 500×) of films (glass + conductive component with volume concentration v): glass A + $Bi_2Ru_2O_7$ (v = = 0.1470) and glass B + RuO_2 (v = 0.1480). On the micrographs the conductive component is white, glass is grey and the pores are black. Fig. 3 shows the effect of frit grain size on the structure of films based on $Bi_2Ru_2O_7$ (v = 0.1802) fired at peak temperatures of 600 and 850 °C respectively. All the four sorted fractions of glass frit A, dealt with in the paragraph on experimental materials, were used in the preparation of pastes for printing these films. A more detailed view of the TFR structure, particularly of the mutual movement (redistribution) of conductive grains in the course of firing is demonstrated by scanning electron micrographs (magn. 2500×) of the B + RuO_2 films (v = 0.1481) fired at several peak temperatures (Fig. 4).

The structure of crystalline components

X-ray diffraction on the fired films proved the formation of admixtion bismuth-lead ruthenates [6] in films based on the $Bi_2Ru_2O_7$ conductive component, with both types of glass, A and B. After firing, the combination of $Bi_2Ru_2O_7$ with glass A showed a small amount of RuO_2 which, however, was not found in the combination with glass B. The amount of Pb entering the lattice of $Bi_2Ru_2O_6$ increases with firing temperature, as indicated by the dependence of the lattice parameter on firing temperature t_v in Fig. 5. The value of the lattice parameter of $Bi_2Ru_2O_7$ is given

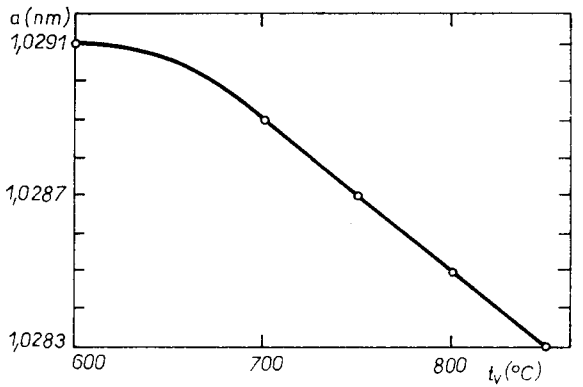

Fig. 5. Dependence of the lattice parameter of the pyrochloric structure of the conductive component in the $Bi_2Ru_2O_7$ films with glass A on firing temperature.

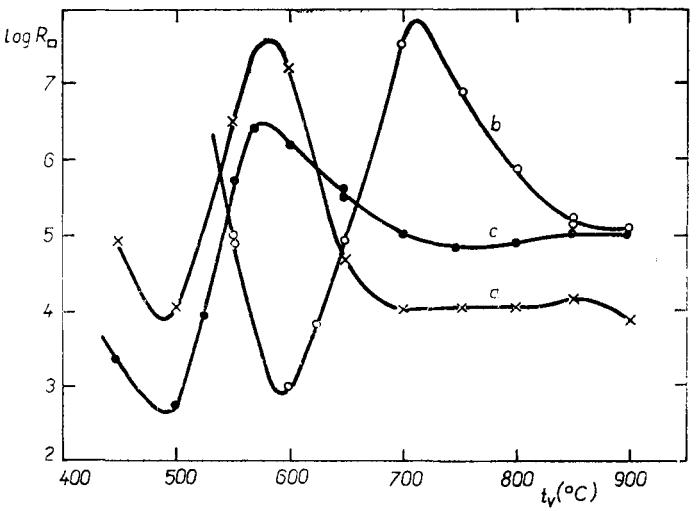

Fig. 6. Dependence of area resistivity on firing temperature of films a — $Bi_2Ru_2O_7$ with glass B (v = 15.69 vol. %), b — RuO_2 with glass A (v = 13.68 vol. %), c — RuO_2 with glass B (v = 14.81 vol. %).

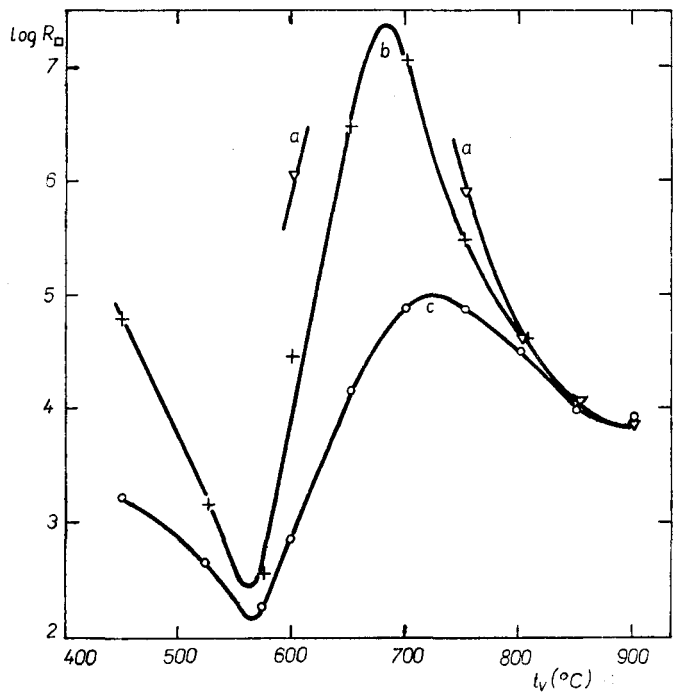

Fig. 7. Area resistivity vs. firing temperature of $Bi_2Ru_2O_7$ films with sorted glass A particle size fractions; a — A(2.24), b — A(1.17), c — A(0.51).

as $a = 1.0288 \pm 0.00095$ nm [15], and 1.0299 nm [14], and measurements on 8 different samples of the powdered compound $Bi_2Ru_2O_7$, carried out at our Institute, yielded the value $a = 1.0290 \pm 0.0002$ nm [17]. For $Pb_2Ru_2O_6$, the same authors

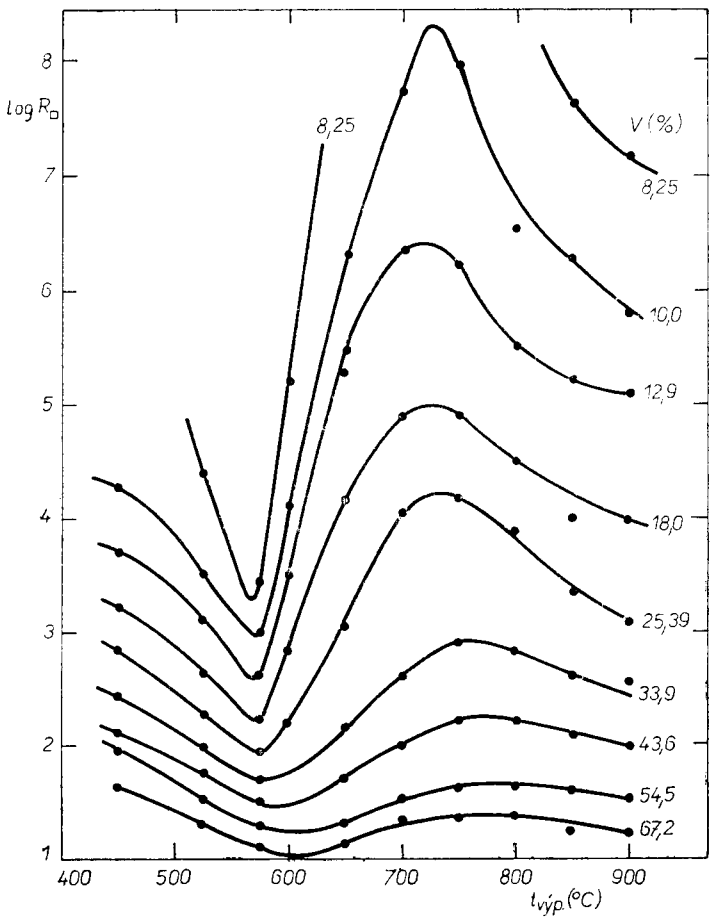

Fig. 8. The effect of concentration of the $Bi_2Ru_2O_7$ conductive component on the course of dependence of area resistivity on firing temperature of films containing glass A(0.51).

found $a = 1.0254$ nm [17], and $a = 1.0253 \pm 0.0002$ nm [18]. Ruthenium oxide only was found in RuO_2 — based films, and no formation of $Pb_2Ru_2O_6$ was observed contrary to the results of [6].

Area resistivity

The dependence of area resistivity on peak temperature was studied for two main reasons. In the first place because it is the basic parameter of TFR and in the second the course of the $R(t_v)$ relationship was shown to supplement very suitably the

structural examination described above. The results of measuring the courses of $R(t_v)$ for three different systems of model TFR are plotted in Fig. 6. The shape of the dependence is essentially determined by processes taking place in the formation of the film structure, and the positions of the individual peaks on the ordinate of firing temperatures are closely associated with the properties of the glass. The actual shape of the dependence $R(t_v)$ is also affected by additional parameters, above all by the grain size of both components and the concentration of the conductive pigment. Fig. 7 demonstrates the influence of the glass frit grain size and Fig. 8 that of the concentration of the conductive components over the wide interval from 8.25 to 67.2 vol. % of $Bi_2Ru_2O_7$ with glass *A* (0.51). Both parameters, as indicated by the diagrams, affect particularly the values of area resistivity at both extremes (minimum and maximum) and at the same time also influence the position of extremes along the firing temperature ordinate.

DISCUSSION

The mechanisms taking part in the development of the TFR structure considered on the basis of microscopic examinations and electrical measurements do not essentially differ from the concepts published earlier [7—9, 15] as regards the initial stages of firing. However, the present authors have a quite different idea of the final stage during which the structure of the resistor film is formed and which decisively influences the mechanism of charge transport in TFR. In the simplest way, this idea of the development of TFR structure can be described by the following steps:

a) sintering of glass,

b) wetting of the conductive particles with glass and their rearrangement under the effect of capillary forces,

c) diffusion of Ru from conductive particles into glass.

In Fig. 9 the individual mechanisms acting during the formation of the film structure are schematically adjoined to the individual sections of the dependence of area resistivity on firing temperature. A similar course is exhibited by the rela-

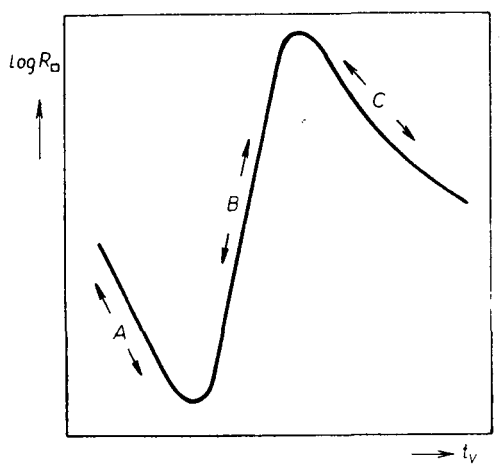

Fig. 9. Schematic attribution of the mechanisms controlling the structural development of TFR to sections on the curve describing the dependence of area resistivity on firing temperature.

tionship between the resistivity measured in the course of firing during the passage of the specimen through the kiln [15]. The division into the individual sections in Fig. 9 is only approximate, as the neighbouring mechanisms very likely overlap.

The development of structure in the course of firing begins by the burning out of the organic vehicle, which takes place virtually completely at temperatures of up to 450 °C. The course of the next two stages of structural development depends above all on the properties of the glass employed (viscosity, surface tension), grain sizes of the two components and to a lesser degree on the concentration of the conductive pigment.

a) Sintering of glass

The sintering of glass frit is effected by Newtonian viscous flow as shown e.g. in [7—9]. In the initial stages, the rate of sintering expressed as a time change in shrinkage, is given by equation [20]:

$$\frac{\mathrm{d}}{\mathrm{d}t}\left(\frac{\Delta L}{L_0}\right) = \frac{3}{4}\frac{\gamma_{sv}}{\eta} D^{-1}, \tag{2}$$

where $\Delta L/L_0$ is the relative change in the distance between the centres of neighbouring particles, γ_{sv} is the solid-vapour interfacial energy, η is viscosity and D, is the mean diameter of the glassy particles. The films show shrinkage virtually in the direction of thickness, as the other two dimensions have been fixed by adhesion to the substrate since the initial stages of firing. The course of shrinkage is indicated by the initial part of the dependence of film thickness on firing temperature in Fig. 10. Comparison with the course of relationship between area resistivity and firing temperature (Fig. 9) shows a connection between the glass frit sintering and decreasing resistivity in region A. The sintering of glass is likewise well discernible on the micrographs. The process of sintering is virtually restricted to this region A. The sintering of glass and film shrinkage result in a compression of the conductive pigment grains and thus in reduced contact resistivity between them, in an increase in the density of conductive particles in the regions between the glass grains and thus in an increase in the electrical conductivity of the film. The granulometric composition of the glass grains remains virtually unchanged in this region and the conductive pigment is distributed among them or over their surface. In materials with mean glass particle size substantially larger then the mean size of conductive grains this stage of firing leads to a typical segregated structure, as defined in the introduction (Fig. 3). The resistivity value at the minimum of the area resistivity vs. firing temperature curve depends on the volume concentration of the conductive component as well as on the ratio of mean dimensions of the glass grains and the conductive ones. The larger the ratio, the smaller the resistivity of the film with a segregated structure [19], as also demonstrated by Fig. 7. According to equation (2), the grain size of the glass grains likewise affects the rate of sintering. This is why the position of area resistivity minimum shifts towards the higher firing temperatures with increasing mean glass grain diameter (with decreasing BET of the specific area). According to the present concept of the consequences of glass sintering, the conductance of electric current through a specimen is provided by direct contacts between the conductive grains. This is also in agreement with the sign of Seebeck's coefficient of films prepared at firing temperatures corresponding to the resistivity minimum, which is identical with the sign given for $Bi_2Ru_2O_7$ (Fig. 12). In studies [14, 21], the Seebeck's coefficient value of $Bi_2Ru_2O_7$ is given as $\alpha = -7\ \mu VK^{-1}$.

b) Wetting of conductive particles and their rearrangement

The viscosity of the glass melt decreases with increasing temperature to such a degree that in the relatively short time of firing the surface of conductive grains is wetted and moreover, the capillary forces drive the glass melt between the conductive grains, thus changing their arrangement in the film [22]. The height h to which the liquid phase penetrates between the solid particles is given for the time-independent contact angle Θ by equation (3) according to [23]:

$$h^2 = \frac{r\gamma_{LV}}{2\eta} \cos \Theta . t \qquad (3)$$

where r is the capillary radius,

γ_{LV} is the solid-liquid interfacial energy.

The mechanism of wetting the surface of conductive particles with glass melt and the effects of capillary forces are responsible for the transition from the segregated structure to a quasihomogeneous one. On the micrographs, this development shows best on specimens with larger glass grains in the paste (Figs. 1 through 4). In agrement with equation (3) a better homogeneity of conductive particle distribution is achieved by firing at the same temperature with films of lower viscosity. According to their definitions, the segregated and quasihomogeneous structures are limit cases of the TFR structure. However, morphology of a number of fired films represents a transition between these limit cases and is characteristic particularly of glass regions free of conductive pigment and resulting from the larger glass grains in the paste. This type of structure will be called intermediate structure. With many films, this intermediate structure persists up to relatively high firing temperatures (Figs. 1 and 3), in dependence on the glass frit grain size distribution and the parameters of the glass. Deviations from an ideal distribution of conductive particles in the glassy

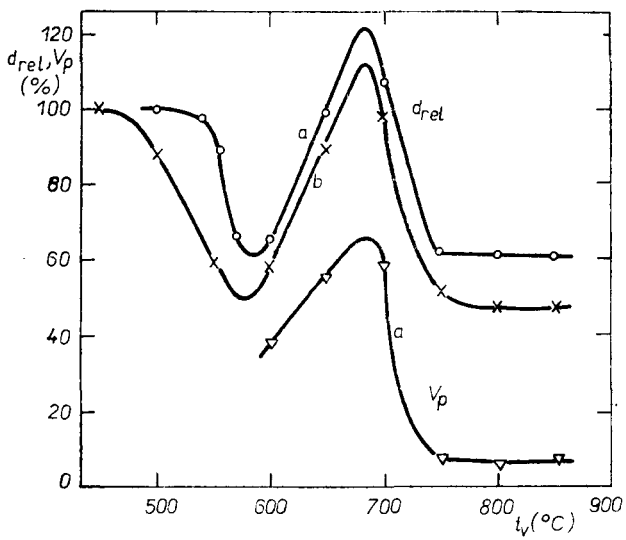

Fig. 10. Relative film thicknesses and volume percent of pores vs. the firing temperature of films; a — $Bi_2Ru_2O_7$ with glass A, b — glass A free from the conductive component.

matrix of the film forming the intermediate structure affect the concentration dependence of resistivity, particularly the value of critical concentration, the percolation limit [25].

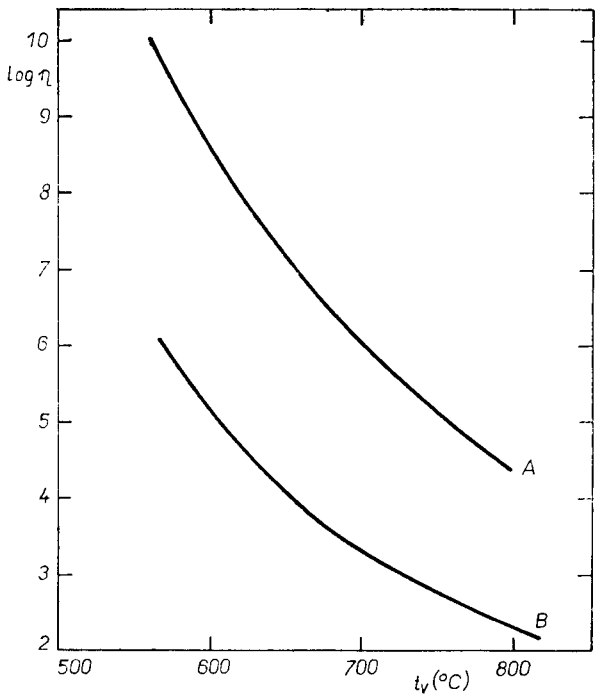

Fig. 11. Viscosity of glasses A and B vs. temperature [27].

The percolation limit is that concentration of conductive paticles at which the opposite sides of the specimen become conductively connected.

The stage of structural development discussed in this paragraph is often accompanied by liberation of gases from the melt and formation of bubbles, as seen in the diagram in Fig. 10 and the micrographs in Figs. 1 and 2. The liberation of gases, the ascent of bubbles towards the layer surface and their growth due to joining of smaller pores and an increases in gas pressure inside the bubble, all take place with decreasing glass viscosity at rising temperature of firing. The growth of bubbles results in an increase in the film volume, which means an increases in thickness, as demonstrated by Fig. 10. The similarity of the courses of the pore content (Fig. 10) and area resistivity (Figs. 6 through 8) on firing temperature is due to the fact that the formation and growth of pores depends above all on the viscosity of the glass just as on the wetting of the surface of conductive particles. The presence of pores in the film cannot cause the resistivity to increase by several orders as a result of change in the geometrical factor in the expression for resistivity. For the sake of illustration, Fig. 13 shows an example of pore distribution. The individual micrograpths taken at one and the same point of the specimen were obtained during gradual diminishing of the film thickness by grinding.

c) Diffusion of Ru from conductive particles into glass

In contrast to studies [7 through 9, 15, 23] the present authors do not consider sintering of conductive particles as a necessary prerequisite for the conductivity of TFR with a quasihomogeneous or intermediate structure, for the following reasons:

1. In the studies quoted, no evidence was presented for the sintering of conductive particles during the firing of TFR; conversely, in [9] it is concluded that no direct evidence by microscopic methods is possible owing to the small dimensions of the conductive particles.

2. The low critical concentrations of the conductive phase (low values of the conduction threshold), found with TFRs of quasihomogeneous or intermediate structures [25] would require arrangement of the conductive particles in chains, and this is in disagreement with the effects of the mechanism discussed in article b).

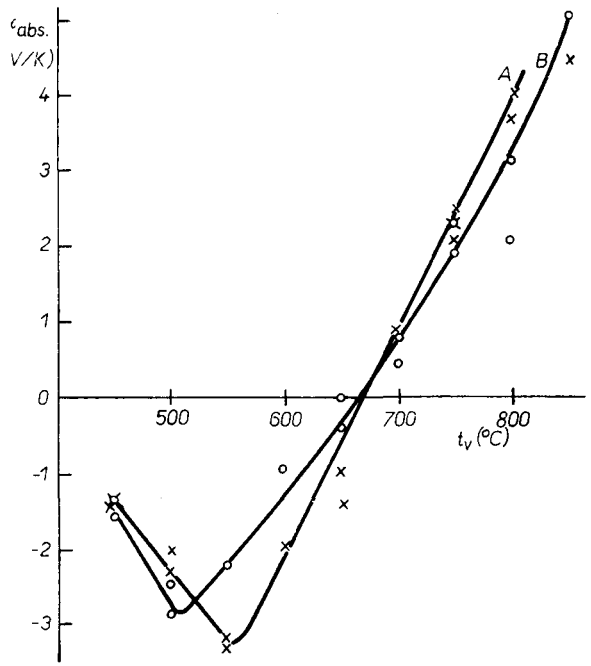

Fig. 12. Absolute Seebeck's coefficient vs. firing temperature of $Bi_2Ru_2O_7$ *films with glasses A and B.*

3. The change in the sign of Seebeck's coefficient (Fig. 12) indicates to a change in the decisive conductivity mechanism.

4. The results of measurements of the frequency dependence of complex conductivity components agree very well with the theory based on the assumption of transport within the narow band of localized states near the Fermi level [13].

In the suggested model of the development of TFR structure the basic idea is therefore that at higher firing temperatures there is a non-negligible diffusion of Ru from the surface of conductive grains into the glassy matrix, and thus localized impurity states are formed in the disarranged structure of glass, which allows transport of electrons by phonon-assisted tunnelling [13]. RuO_2 is not a glass-forming oxide,

and dissolves therefore very little in glasses [9, 26]. The creation of concentration of localized states satisfactory for transport of electrons by the mechanism mentioned results from the small distances between the conductive grains.

CONCLUSION

As follows from the account given above, the development of the structure of TFR in the course of film firing can be described to take place in the following three steps:

1. The sintering of glass.

2. The wetting of conductive particles with glass melt and their spreading by capillary forces.

3. Diffusion of Ru into glass and formation of a narrow band of localized impurity states.

The mechanisms given in points 1 and 2 agree essentially with the literature [7—9], but the present model shows a basic difference from the results of the quoted studies at point 3, describing the last stage of structural formation in most TFR films: according to the suggested conception, formation of a band of localized levels by diffusion of Ru into glass, instead of the earlier assumed sintering of conductive particles into chains. Our model is supported by the results of measuring Seebeck's coefficient and the frequency dependences of impedance components [13].

The authors wish to express their thanks to Concern Corporation TESLA Lanškroun and particularly to ing. J. Burša for his support of, and interest in the studies in question. The authors are also indebted to B. Diskočilová, B. Stará for technical assistance and to V. Štefek for his scanning electron micrographs.

References

[1] Bigers J. V., McKelvy J. R., Schulze W. A.: J. Amer. Cer. Soc. *65*, C-13 (1982).
[2] Inokuma T., Taketa Y., Haradome M.: IEEE Trans. on Comp., Hybrids and Manuf. Technol. *CHMT-7*, 166 (1984).
[4] Prudenziati M.: Electrocomp. Sci. Technol. *10*, 285 (1983).
[5] Ewen P. J. S., Robertson J. M.: J. Phys. D: Appl. Phys. *14*, 225 (1981).
[6] Hofman L. C.: ACS Bull. *63*, 572 (1984).
[7] Palanisamy P.: PhD Thesis, Purdue Univ., West Lafayette, 1979.
[8] Tarn C. T.: PhD Thesis, Purdue Univ., West Lafayette, 1979.
[9] Prabhu A. N., Vest R. W.: Mater. Sci. Res. *10*, 399 [1975).
[10] Cattaneo A., Prudenziati M.: Electrocomp. Sci. Technol. *6*, 165 (1980).
[11] Prudenziati M., Morten B., Masoero A.: J. Phys. D: Appl. Phys. *14*, 1355 (1981).
[12] Lee J., Vest R. W.: IEEE Trans. on Comp., Hybrids and Manuf. Technol. *CHMT-6*, 430 (1983).
[13] Kubový A., Stefan O.: Thin Solid Films *135*, L9 (1986).
[14] Bouchard R. J., Gillson J. L.: Mater. Res. Bull. *6*, 669 (1971).
[15] Paszczyński S.: Rozpr. Elektrotech. *29*, 217 (1983).
[16] Pike G. E., Seager C. H.: J. Appl. Phys. *48*, 5152 (1977).
[17] Plocek L., Štefková E.: Unpublished results.
[18] Longo J., Raccan P. M., Goodenough J. B.: Mater. Res. Bull. *4*, 191 (1969).
[19] Kubový A.: J. Phys. D: Appl. Phys. *19*, 2171 (1986).
[20] Geguzin Ja. E.: *The Physics of Sintering*, ed. 1 (in Russian), p. 63, Nauka Moscow 1967.
[21] de Jeu W. H., Geukens R. W. J.: J. Appl. Phys. *52*, 4128 (1981).
[22] Huppmann W. J., Rieger H.: Acta Metall. *23*, 965 (1975).
[23] Sarma D. H., Vest R. W.: J. Amer. Cer. Soc. *68*, 249 (1985).
[24] Palanisamy P., Sarma D. H. R., Vest R. W.: J. Amer. Cer. Soc. *69*, C-215 (1986).
German R. M.: J. Amer. Cer. Soc. *69*, C-40 (1986).
[25] Kubový A.: To be published.
[26] Sartain C. C., Ryden W. D., Lawson A. W.: J. Non-Crystal. Solids *5*, 55 (1970).
[27] Broukal J.: Private communication.

VLIV TEPLOTY VÝPALU NA VLASTNOSTI MODELOVÝCH TLUSTOVRSTVÝCH REZISTORŮ

I. Morfologie a mikrostruktura vrstev

Alois Kubový, Ivo Havlas

Výzkumný ústav elektrotechnické keramiky, 500 64 Hradec Králové

Cílem práce bylo vypracování modelu vývoje struktury modelových tlustovrstvých rezistorů během jejich výpalu. Použité modelové pasty, na rozdíl od komerčních, neobsahovaly ve své anorganické složce kromě vodivého pigmentu a mleté skleněné frity žádné modifikující oxidy ani další dopanty. Vliv teploty výpalu v tunelové peci byl sledován v intervalu vrcholových teplot od 450 do 900 °C s výdrží 9 min. na maximální teplotě. Byly studovány pasty s kombinacemi vodivé složky $Bi_2Ru_2O_7$ nebo RuO_2 se sklem *A* nebo *B*, jejichž složení a BET měrný povrch uvádí tab. I. Část výsledků byla získána studiem vrstev připravených se skelnou fritou složení *A*, která byla po mletí tříděna na 4 granulometrické frakce.

Návrh modelu je podložen mikroskopickými vyšetřeními optickým i elektronovým rastrovacím mikroskopem a měřením plošných resistivit a Seebeckova koeficientu. Z výsledků experimentů vyplynulo, že vývoj struktury lze rozdělit do tří kroků:

1. sintrování skla;
2. smáčení vodivých částic sklovinou a jejich rozdružování kapilárními silami;
3. difúze Ru do skla a vznik úzkého pásu lokalizovatelných příměsových stavů.

Uvedené výsledky se od dříve publikovaných prací [7 až 9, 15, 24] zásadně liší v bodě 3 tím, že se předpokládá místo dříve uváděného sintrování vodivých částic vznik pásu příměsových hladin. Náš model je podpořen zejména výsledky měření Seebeckova koeficientu a dříve publikovaných kmitočtových závislostí složek impendance [13].

Obr. 1. Odleštěné povrchy vrstev $Bi_2Ru_2O_7$ *se sklem A pálených při různých vrcholových teplotách, v = 14,70 obj. %; a — 600 °C, b — 700 °C, c — 900 °C.*

Obr. 2. Odleštěné povrchy vrstev RuO_2 *se sklem B pálených při různých vrcholových teplotách, v = 14,80 obj. %; a — 500 °C, b — 600 °C, c — 800 °C.*

Obr. 3. Vliv velikosti zrna skleněné frity A (různým měrným povrchem) na morfologii vrstev s vodivou složkou $Bi_2Ru_2O_7$, *v = 18,02 obj. %, t_v = 600 °C; a — 2,24 m²/g, b — 0,78 m²/g, c — 0,51 m²/g, t_v = 850 °C: d — 2,24 m²/g, e — 0,78 m²/g, f — 0,51 m²/g.*

Obr. 4. Mikrosnímky z rastrovacího elektronového mikroskopu vrstev RuO_2 *se sklem B pálených při různých vrcholových teplotách; v = 14,81 obj. %; a — 550 °C, b — 600 °C, c — 700 °C.*

Obr. 5. Závislost mřížkového parametru pyrochlorové struktury vodivé složky vrstev $Bi_2Ru_2O_7$ *se sklem A na teplotě výpalu.*

Obr. 6. Závislosti plošné resistivity na teplotě výpalu vrstev a — $Bi_2Ru_2O_7$ *se sklem B (v — 15,69 obj. %), b —* RuO_2 *se sklem A (v = 13,68 obj. %), c —* RuO_2 *se sklem B (v = 14.81 obj. %).*

Obr. 7. Závislosti plošné resistivity na teplotě výpalu vrstev $Bi_2Ru_2O_7$ *s tříděnými frakcemi skla A; a — A(2,24), b — A(1,17), c — A(0,51).*

Obr. 8. Vliv koncentrace vodivé složky $Bi_2Ru_2O_7$ *na průběh závislosti plošné resistivity na teplotě výpalu vrstev se sklem A(0,51).*

Obr. 9. Schematické přiřazení mechanismů řídících vývoj struktury TFR úsekům na křivce závislosti plošné resistivity na teplotě výpalu.

Obr. 10. Relativní tloušťky vrstev a objemové procento pórů proti teplotě výpalu vrstev; a — $Bi_2Ru_2O_7$ *se sklem A, b — sklo A bez vodivé složky.*

Obr. 11. Závislosti viskozity skel A a B na teplotě [27].

Obr. 12. Závislost absolutního Seebeckova koef. na teplotě výpalu vrstev $Bi_2Ru_2O_7$ *se skly A a B.*

Obr. 13. Mikroskopické snímky vrstvy $Bi_2Ru_2O_7$ *se sklem A(0,51),* t_v *= 700 °C, v = 18,02 obj. % postupně odbrušované z původní tloušťky 46,7 μm — na tl. 35 μm — b, 11,7 μm — c a 6,8 μm — d.*

ВЛИЯНИЕ ТЕМПЕРАТУРЫ ОБЖИГА НА СВОЙСТВА МОДЕЛЬНЫХ ТОЛСТОПЛЕНОЧНЫХ РЕЗИСТОРОВ

I. Морфология и микроструктура слоев

Алоис Кубовы, Иво Гавлас

Научно-исследовательский институт электротехнической керамики
500 64 Градец Кралове

Целью предлагаемой работы является разработка развития структуры модельных толстопленочных резисторов в течение их обжига. Применяемые модельные пасты, в отличие от паст, находящихся в продаже, не содержат в своем неограническом компоненте, кроме проводящего пигмента и молотой стеклянной фритты, никакие модифицирующие оксиды и никакие дальнейшие добавки. Влияние температуры обжига в туннельной печи исследовали в интервале пиковых температур в пределах от 450 до 900 °C с выдержкой 9 мин. на максимальной температуре. Исследовали пасты с комбинациями проводящего компонента $Bi_2Ru_2O_7$ или RuO_2 со стеклом A или B, состав и BET удельная поверхность, которых приводится в табл. I. Часть результатов получали, исследуя слои, приготовленные с помощью стеклянной фритты составом A, которую после помола разделили в четыре гранулометрические фракции.

Предложение модели основывается на микросокпическом исследовании, проводимом с помощью оптического и электронного сканирующего микроскопа и на измерении поверхностного удельного сопротивления и коэффициента Сеебека. Из результатов экспериментов следует, что развитие структуры можно подразделить в три этапа:

1. спекание стекла,
2. смачивание проводящих частиц стекломассой и их разделение капилярными силами,
3. диффузия Ru в стекло и образование узкой полосы локализованных примесных состояний.

Приводимые результаты принципиально отличаются в 3 пункте от до сих пор опубликованных работ [7—9, 15, 24] в том смысле, что вместо ранее приводимого спекания проводящих частиц учитывается образование полосы примесных уровней. Предполагаемая нами модель доказывается именно результатами измерения коэффициента Сеебека и ранее опубликованными частотными зависимостями компонентов импеданса [13].

Рис. 1. Отполированные поверхности слоев $Bi_2Ru_2O_7$ со стеклом A, обжигаемых при разных пиковых температурах, v = 14,70 % по объему; a — 600 °C, b — 700 °C, c — 900 °C.

Рис. 2. Отполированные поверхности слоев RuO_2 со стеклом B, обжигаемых при разных пиковых температурах, v = 14,80 % по объему; a — 500 °C, b — 600 °C, c — 800 °C.

Рис. 3. Влияние размера зерна стеклянной фритты A (с разной удельной поверхностью) на морфологию слоев с проводящим компонентом $Bi_2Ru_2O_7$, v = 18,02 % по объему, t_v = 600 °C; a — 2,24 м²/г, b — 0,78 м²/г, c — 0,51 м²/г.

Рис. 4. Микросъемки из сканирующего электронного микроскопа слоев RuO_2 со стеклом B, обжигаемых при равных пиковых температурах, v = 14,81 % по объему: a — 550 °C, b — 600 °C, c — 700 °C.

Рис. 5. Зависимость решеточного параметра пирохлорной структуры проводящего компонента слоев $Bi_2Ru_2O_7$ со стеклом A от температуры обжига.

Рис. 6. Зависимость поверхностного удельного сопротивления от температуры обжига слоев a — $Bi_2Ru_2O_7$ со стеклом B (v — 15,69 % по объему), b — RuO_2 со стеклом A (v = 13,68 % по объему), c — RuO_2 со стеклом B (v — 14,81 % по объему).

Рис. 7. Зависимость поверхностного удельного сопротивления от температуры обжига слоев $Bi_2Ru_2O_7$ с разделенными фракциями стекла A; a — A(2,24), b — A(1,17), c — A(0,51).

Рис. 8. Влияние концентрации проводящего компонента $Bi_2Ru_2O_7$ на ход зависимости поверхностного удельного сопротивления от температуры обжига слоев со стеклом A (0,51).

Рис. 9. Схематическая координация механизмов, управляющих развитием структуры TFP относительно отрезков на кривой зависимости поверхностного удельного сопротивления от температуры обжига.

Рис. 10. Относительные толщины слоев и процент пор по объему относительно температуры обжига слоев; а — $Bi_2Ru_2O_7$ со стеклом А, b — стекло А без проводящего компонента.

Рис. 11. Зависимость вязкости стекол А и В от температуры [27].

Рис. 12. Зависимость абсолютного коэффициента Сеебека от температуры обжига слоев $B_2Ru_2O_7$ со стеклами А и В.

Рис. 13. Микроскопические съемки слоя $Bi_2Ru_2O_7$ со стеклом А(0.51), $t_v = 700$ °C, $v = 18{,}02$ % по объему постепенно отполированные с исходной толщины 46,7 μм до толщины 35 μм — b, 11,7 μм — c и 6,8 μм — d.

SPEVŇOVANIE KERAMIKY NA BÁZE Si_3N_4 POUŽITÍM SiC VISKROV sa ukazuje ako jedna z možností prípravy vyspelej keramiky s vysokou lomovou húževnatosťou. V práci japonských autorov K. UENA a S. SODEOKA (Yogyo-Kyokai-Shi, *94* (1986) 981) sa uvádza, že keramika s obsahom 15 hm. % SiC viskrov má koeficient lomovej húževnatosti $K_{IC} = 7{,}2$ MN $m^{-3/2}$, pričom keramika na báze čistého Si_3N_4 dosahuje maximálnych hôdnot $K_{IC} = 6{,}3$ MN $m^{-3/4}$. Mikroskopické pozorovania naznačujú, že šírenie trhlín v takejto dvojkomponentnej keramike je často zabraňované viskrami a trhliny sú presmerované do medzivrstvy medzi matricou a viskrami. Tento odklon trhlín je možné prisúdiť existencii napätí spôsobených rozdielnou tepelnou roztažnosťou matrixu a viskrov.

P. Šajgalík

NOVÁ TECHNOLÓGIA SPEKANIA — PAS (Pressure Assisted Sintering) je ekonomicky výhodná technológia kompaktácie na hodnoty blízke teoretickej hustote. Jedná sa o nízkotlakovú modifikáciu vysokoteplotného izostatického lisovania, vhodnú pre výrobky práškovej metalurgie. Princíp spočíva vo využití tlaku pri optimálnych časových a teplotných parametroch (patent USA 4591482). Používaný tlak plnu yje v rozmedzí 7—14 MPa. Výhody sú charakterizované podstatne nižšou cenou zariadenia, kratšími časmi spekania, nízkym rozptylom hutností výrobkov, tvarovou presnosťou po spekaní, nízkym alebo chýbajúcim množstvom prísad čo vedie k vysokým parametrom výrobkov pri ich nižšej cene. Podrobnosti možno získať na adrese: Gorham International Inc., P. O. Box 8, Gorham, ME 04038, USA. (Refractories and Hard Metals, str. 133, september 1986).

Z. Pánek

ELEKTRONICKÝ PRŮMYSL OBJEVIL NĚKTERÉ MÉNĚ ZNÁMÉ PIEZOELEKTRICKÉ MATERIÁLY. Nikdo neupírá prvenství křemenným krystalům jako nejrozšířenějšímu piezoelektriku, ale některé keramické a polymerní materiály nyní porostou v odbytu rychleji. Celkový trh piezoelektrických výrobků v USA se odhaduje na 418 mil. $, do r. 1995 se plánuje růst o 5 % ročně na hodnotu 644 mil. $. Nejrychleji poroste využití polymerů a kopolymerů v čele s polyvinylidenfluoridovými filmy. Dnešní trh činí jen 2 mil. $, během příštích 10 let však poroste o 34 % ročně. Je to spojeno s novými aplikacemi (infračervené detektory, velkorozměrné zobrazovače, senzory v oblasti optovláknových elektrických polí). Pomaleji poroste odbyt piezoelektrické keramiky. Dnešní trh 63 mil. $ dosáhne do r. 1995 výše 148 mil. $, ale růst je velmi závislý na vojenských investicích (elektroakustické generátory signálu, senzory elektrostatického napětí, detektory pro ultrazvukový přenos obrazu). Křemenné krystaly si zachovají rozhodující vliv na trhu, ročně porostou asi o 3 % na 471 mil. $ v r. 1995. V USA je nyní 84 společností, které vyrábějí a dodávají piezoelektrické krystaly a součástky, a 22 společností, které vyrábějí piezoelektrické keramické materiály a prvky. Jen 5 amerických firem se nyní podílí na obchodu s piezoelektrickými polymery a kopolymery.

Eletronic Chem. News *2*, 1987, č. 4, 7)

Doušková